ORGANOMETALLICS

Article

pubs.acs.org/Organometallics

New Highly Active Heteroscorpionate-Containing Lutetium Catalysts for the Hydroamination of Aminoalkenes: Isolation and Structural Characterization of a Dipyrrolidinide−Lutetium Complex

Antonio Otero,*[,†] Agustín Lara-Sánchez,*[,†] Carmen Nájera,[‡] Juan Fernández-Baeza,[†] Isabel Márquez-Segovia,[†] José Antonio Castro-Osma,[†] Javier Martínez,[†] Luis F. Sánchez-Barba,[†] and Ana M. Rodríguez[†]

[†]Departamento de Química Inorgánica, Orgánica y Bioquímica, Universidad de Castilla-La Mancha, 13071-Ciudad Real, Spain

[‡]Departamento de Química Orgánica, Facultad de Ciencias, and Instituto de Síntesis Orgánica (ISO), Universidad de Alicante, Apdo 99, 03080-Alicante, Spain

Supporting Information

ABSTRACT: The reactions of the hybrid scorpionate/cyclopentadiene compounds, as a mixture of regioisomers—1-[2,2-bis(3,5-dimethylpyrazol-1-yl)-1,1-diphenylethyl]-1,3-cyclopentadiene and 2-[2,2-bis(3,5-dimethylpyrazol-1-yl)-1,1-diphenylethyl]-1,3-cyclopentadiene (bpzcpH) and 1-[2,2-bis(3,5-dimethylpyrazol-1-yl)-1-*tert*-butylethyl]-1,3-cyclopentadiene and 2-[2,2-bis(3,5-dimethylpyrazol-1-yl)-1-*tert*-butylethyl]-1,3-cyclopentadiene (bpztcpH)—with $[Lu(CH_2SiMe_3)_3(thf)_2]$ proceed in very high yields to give the free solvent neutral heteroscorpionate dialkyl lutetium complexes $[Lu(CH_2SiMe_3)_2(bpzcp)]$ (**1**) and chiral $[Lu(CH_2SiMe_3)_2(bpztcp)]$ (**2**). The structures in solution of **1** and **2** were investigated by VT NMR spectroscopy, and a fluxional behavior corresponding to an exchange between the alkyl groups was observed. The lutetium complex $[Lu(CH_2SiMe_3)_2(bpztcp)(thf)]$ (**3**) was isolated as an enantiomerically enriched complex. Supramolecular CH−π interactions between molecules in crystals of **3** have been identified in its X-ray molecular analysis, and they explain the formation of a conglomerate among molecules of **3**. Complexes **1**−**3** are efficient catalysts for the intramolecular hydroamination of aminoalkenes, giving TOF values of up to 475 h^{-1} at 90 °C for 2,2-diphenyl-pent-4-enylamine (**4**) by using complex **3** as catalyst. Enantioselectivities up tp 70% ee were achieved in the cyclization of the 1,2-disubstituted olefin **6** with the high enantiopurity complex **3**. The hydroamination reactions show apparently zero-order rate dependence on substrate concentration and first-order rate dependence on catalyst concentration. Additionally, bicyclization of 2-allyl-2-methylpent-4-enylamine (**10**) was achieved at 60 and 100 °C, giving *exo*,*exo*-2,4,6-trimethyl-1-azabicyclo[2.2.1]heptane (**12**). The protonolysis reaction of complex $[Lu(CH_2SiMe_3)_2(bpztcp)]$ (**2**) with 2 equiv of 2,2-diphenyl-pent-4-enylamine (**4**) yielded a dipyrrolidinide lutetium complex $[Lu(NC_4H_5\text{-}2\text{-}Me\text{-}4,4\text{-}Ph_2)_2(bpztcp)]$ (**13**) as a mixture of two diastereoisomers. The structures of the complexes were determined by spectroscopic methods, and the X-ray crystal structures of **3** and **13** were also established.

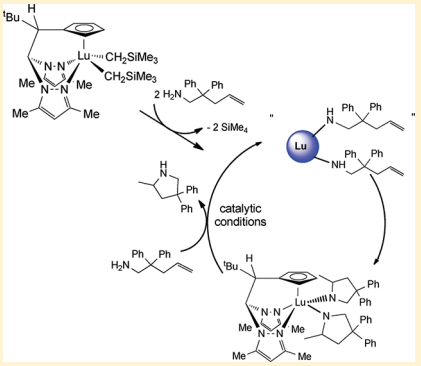

INTRODUCTION

The hydroamination of C−C multiple bonds is a prominent and highly atom-efficient reaction for the synthesis of nitrogen-containing compounds.[1] In particular, the enantioselective intramolecular cyclohydroamination of aminoalkenes or aminoalkynes has applications in the pharmaceutical and fine chemical industries.[2] This catalytic addition of amine N−H functionalities to unsaturated carbon−carbon bonds allows the preparation of complex nitrogen-containing compounds in a waste-free, highly atom-economical manner starting from simple and inexpensive starting materials. A staggering number of catalytic systems have been developed for this reaction, and these exhibit a correspondingly high degree of mechanistic diversity.[1−5] In particular, the intramolecular hydroamination of a variety of carbon−carbon unsaturations such as alkenes, alkynes, allenes, and dienes using group 3 and rare-earth-metal complexes is well documented.[1−6] It has been established that this process involves an intramolecular insertion of the unsaturated substrate into a metal−amido bond,[4i,6] via a four-centered transition state, followed by a rapid protonolysis of the intermediate lanthanide−alkyl species formed by amine substrates to yield the azacyclic product and regenerate the catalytically active species (Figure 1).

The improvement of new transition-metal-based hydroamination catalysts with higher activity and selectivity, including chiral catalysts for enantioselective hydroamination and systems bearing ancillary ligands that permit facile tuning of catalytic properties through adjustment of their steric and electronic features, has remained a challenge.[7] Heteroscorpionates are among the most versatile types of tridentate ligands, and they can coordinate to a wide variety of elements.[8] Chemistry based

Received: November 23, 2011
Published: March 6, 2012

   dx.doi.org/10.1021/om2011672 | *Organometallics* 2012, 31, 2244−2255

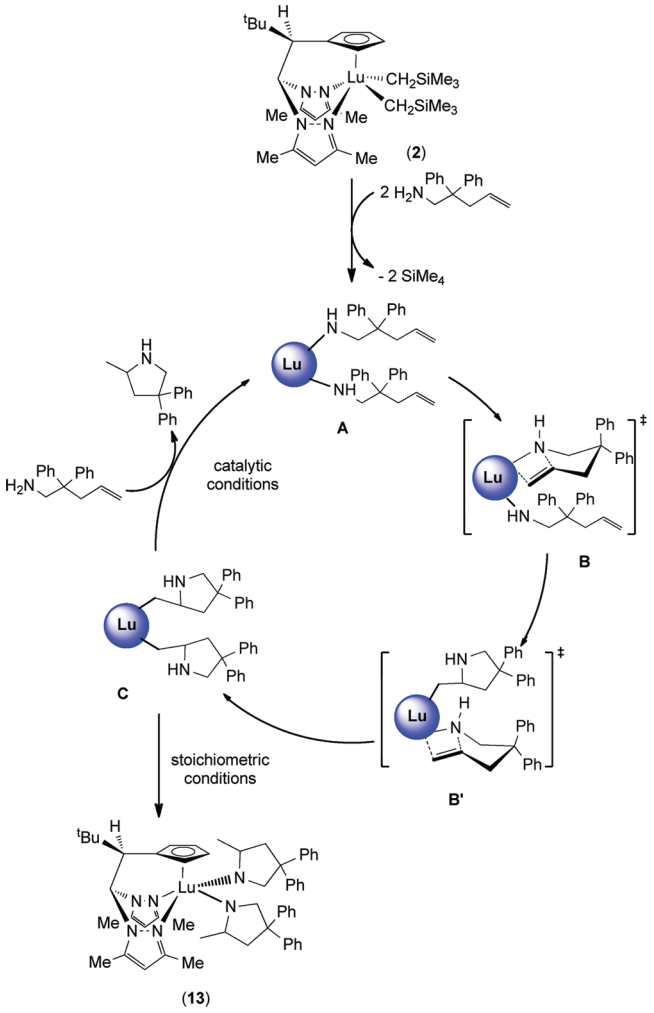

Figure 1. Proposed σ-bond insertion mechanism (diamido) for intramolecular hydroamination.

on the design of this particular type of intriguing ligand has been extended considerably in terms of coordination chemistry[9] and catalytic applications.[10] In the past decade, a number of research groups have contributed widely to this field, designing new ligands related to the bis(pyrazol-1-yl)methane system and incorporating several pendant donor arms.[11] Bearing in mind both the versatility of this type of tridentate monoanionic ligand and the efficiency of rare-earth-catalyzed hydroamination, we decided to develop hydroamination catalysts based on heteroscorpionate ligands. It was envisaged that these compounds would have catalytic activity comparable to that of the lanthanocene systems.

Herein, we describe in detail the synthesis and characterization of a series of achiral and chiral heteroscorpionate alkyl lutetium complexes, one of them enantiomerically enriched, and the first X-ray characterized dipyrrolidinide rare-earth complex. The performance of those complexes in the hydroamination/cyclization of aminoalkenes was explored under well-controlled conditions.

RESULTS AND DISCUSSION

Syntheses and Structural Characterization. The synthesis of the lutetium dialkyl complexes $[Lu(CH_2SiMe_3)_2(bpzcp)]$ (**1**; bpzcp = 2,2-bis(3,5-dimethylpyrazol-1-yl)-1,1-diphenylethylcyclopentadienyl) and $[Lu(CH_2SiMe_3)_2(bpztcp)]$ (**2**; bpztcp = 2,2-bis(3,5-dimethylpyrazol-1-yl)-1-*tert*-butylethylcyclopentadienyl) was achieved through a protonolysis reaction involving alkane elimination. Thus, the reaction of bpzcpH and *rac*-bpztcpH (see Figure S1 in the Supporting Information), as a mixture of two regioisomers, bpzcpH = 1-[2,2-bis(3,5-dimethylpyrazol-1-yl)-1,1-diphenylethyl]-1,3-cyclopentadiene and 2-[2,2-bis(3,5-dimethylpyrazol-1-yl)-1,1-diphenylethyl]-1,3-cyclopentadiene and bpztcpH = 1-[2,2-bis(3,5-dimethylpyrazol-1-yl)-1-*tert*-butylethyl]-1,3-cyclopentadiene and 2-[2,2-bis(3,5-dimethylpyrazol-1-yl)-1-*tert*-butylethyl]-1,3-cyclopentadiene,[10d] with $[Lu(CH_2SiMe_3)_3(thf)_2]$[12] in a 1:1 molar ratio in toluene at 0 °C yielded the lutetium dialkyl complexes **1** and **2**, respectively, after the appropriate workup procedure, as white solids in ca. 80% yield (Scheme 1). Complex **2** was obtained as a racemic mixture.

Scheme 1. Synthesis of Lutetium Dialkyl Complexes 1 and 2

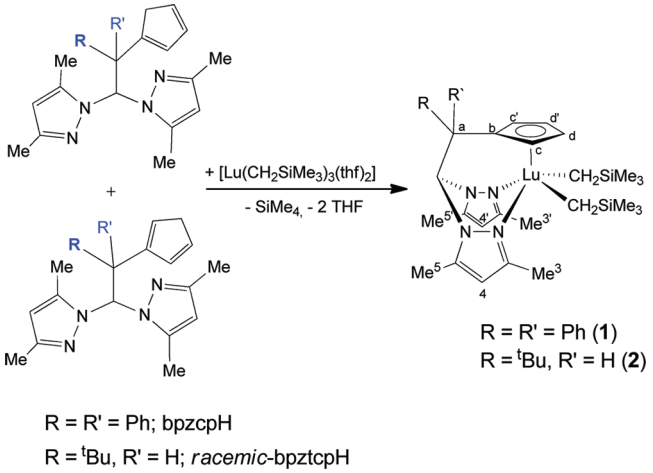

After the preparation of these complexes, we have considered as a new challenge the preparation from *rac*-bpztcpH and $[Lu(CH_2SiMe_3)_3(thf)_2]$ of a related complex to **2** but enantiomerically enriched. With this aim in mind, we are tried to isolate an enantiopure alkyl lutetium complex by diffusion of a toluene solution of racemic heteroscorpionate precursor bpztcpH in hexane solution of $[Lu(CH_2SiMe_3)_3(thf)_2]$ and allowed the solution to crystallize slowly without stirring.[13] Thus, by using this procedure we have able to isolate the dialkyl complex $[Lu(CH_2SiMe_3)_2(bpztcp)(thf)]$ (**3**) enantiomerically enriched by spontaneous resolution and preferential crystallization of one enantiomer due to the preferential formation of a conglomerate (see below their X-ray crystal structure discussion). Complex **3** was obtained as a crystalline colorless solid in ca. 35% yield from the reaction mixture (Scheme 2). It is known that crystallization constitutes the most economical procedure to obtain enantiopure compounds from racemic mixtures, when the separation of the crystals of an enantiomer due to the formation of a conglomerate is feasible.[14] However, in ordered three-dimensional crystals the formation of a conglomerate is not very frequent (and is even less predictable), reflecting the tremendous preference (more than 90%) of compounds to crystallize in centrosymetric space group.[15]

The alkyl complexes **1**–**3** were characterized spectroscopically. The ^1H and $^{13}C\{^1H\}$ NMR spectra at room temperature of **1** (nonchiral compound) exhibit a singlet for each of the H^4, Me^3, and Me^5 pyrazole protons, indicating that the pyrazole rings are equivalent, alongside two multiplets for the

dx.doi.org/10.1021/om2011672 | Organometallics 2012, 31, 2244–2255

Scheme 2. Synthesis of Lutetium Dialkyl Complex 3 Enantiomerically Enriched

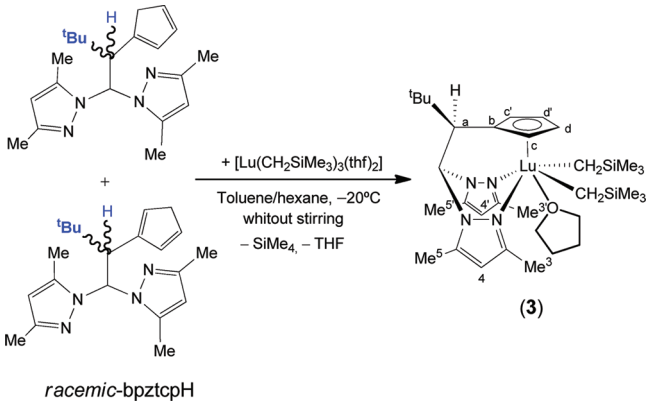

cyclopentadienyl protons and one set of signals for the alkyl groups. A five-coordinate environment for this complex can be proposed for which a symmetric plane exists: i.e., a square-planar-pyramidal geometry (see Scheme 1). However, the ^{1}H and ^{13}C{^{1}H} NMR spectra at room temperature of complexes **2** and **3** (chiral compounds) show two singlets for each of the H^{4}, Me^{3}, and Me^{5} pyrazole protons, four multiplets for the cyclopentadienyl protons, and one set of signals for the alkyl groups along with two multiplets for the THF protons in complex **3**. Additionally, the methylene protons of complexes **2** and **3**, LuCH_2SiMe$_3$, are diastereotopic, giving rise to an AB system (see Figures S3 and S4 in the Supporting Information), due to the stereogenic carbon, C^{a}, from the heteroscorpionate ligand. These results are consistent with a proposed five-coordinate disposition for the complex **2** and an octahedral structural disposition for the complex **3** (see Schemes 1 and 2). Thus, these spectroscopic data indicate that the hybrid scorpionate/cyclopentadienyl ligands are coordinated in a facial, "tripodal" fashion with a κ^2-NN-η^5-Cp coordination mode. The phase-sensitive ^{1}H NOESY-1D NMR spectra were also obtained in order to confirm the assignments of the signals for the Me^{3}, Me^{5}, and H^{4} groups of each pyrazole ring. The assignment of the ^{13}C{^{1}H} NMR signals was made on the basis of ^{1}H−^{13}C heteronuclear correlation (g-HSQC) experiments. It is worth noting that the room-temperature ^{1}H NMR spectra of complexes **2** and **3** show one set of resonances for the two nonequivalent CH_2SiMe_3 ligands. This behavior indicates that the two alkyl ligands exchange rapidly at room temperature. The dynamic behavior of complexes **1** and **2** was studied by VT NMR spectroscopy. In the case of complex **1**, with an achiral heteroscorpionate ligand, the VT NMR analysis showed that the resonance of the methylene protons, Lu−CH_2SiMe$_3$, directly bonded to the lutetium center broaden and become resolved into two signals at low temperature, giving rise to an AB system at −70 °C, probably owing to the lack of rotation of the methylene protons at low temperature. A stacked plot of the relevant sections of the variable-temperature ^{1}H NMR spectra of **1** and **2** are shown in Figures 2 and 3.

At room temperature the exchange of the two alkyl groups for **2** occurs and, accordingly, one set of signals appears. When the temperature was decreased to below −80 °C, two set of signals (relative intensities 1:1) were observed for the alkyl groups (see Figure 3). Free-energy values, $\Delta G^{\ddagger}$, for complexes **1** and **2** were calculated[16] from VT NMR studies. Complex **1** has higher activation barriers, with a coalescence temperature

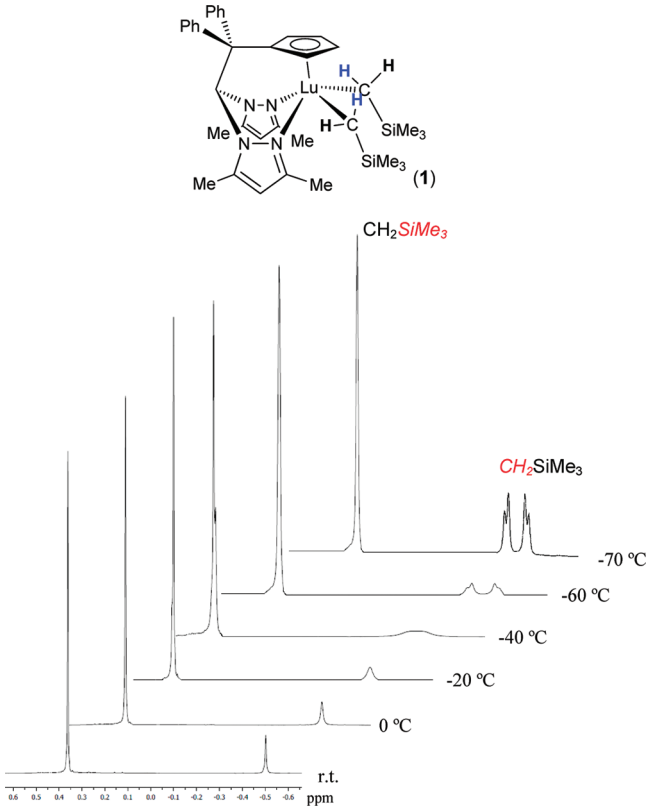

Figure 2. Variable-temperature ^{1}H NMR spectra in the region of the alkyl groups of complex **1**.

of −40 °C and $\Delta G^{\ddagger}$ = 9.2 ± 0.1 kcal/mol, whereas **2** has a coalescence point of −60 °C and $\Delta G^{\ddagger}$ = 8.5 ± 0.1 kcal/mol.

As we have previously commented, complex **3** was isolated enantiomerically enriched by spontaneous resolution and preferential crystallization of one enantiomer. We have tried to confirm the presence in solution of the corresponding two enantiomers in different proportions by adding different chiral shift reagents, but unfortunately the results obtained are not conclusive in order to establish the value of enantiomeric excess (see Figures S3 and S4 in the Supporting Information). Additionally, the value for the specific rotation of complex **3** (see the Experimental Section) is consistent with a enantiomerically enriched complex.

The molecular structure of complex **3** was determined by an X-ray diffraction study. Complex **3** forms a conglomerate that crystallizes in the chiral $P2_1$ space group. This crystal structure was determined by using Mo Kα radiation, and the asymmetric unit contains one independent molecule with the following unit cell dimensions: a = 10.015(5) Å, b = 19.622(3) Å, c = 10.476(2) Å, and β = 114.135(3)°. The crystals are enantiopure with regard to the orientation of the stereogenic carbon, C^{a}, since the molecule in the asymmetric unit has the S configuration (four grains of crystals of the lutetium complex **3** were measured and only S complex **3** was detected). The corresponding ORTEP drawing is depicted in Figure 4. Crystallographic data and selected interatomic distances and angles are given in Tables 1 and 2, respectively. The molecular structure determined by X-ray diffraction is in good agreement with the solution structure deduced from the NMR experiments. The heteroscorpionate ligand is attached to the lutetium atom through the two nitrogen atoms of pyrazole rings and the cyclopentadienyl ring in a κ^2-NN-η^5-Cp coordination mode in

dx.doi.org/10.1021/om2011672 | Organometallics 2012, 31, 2244−2255

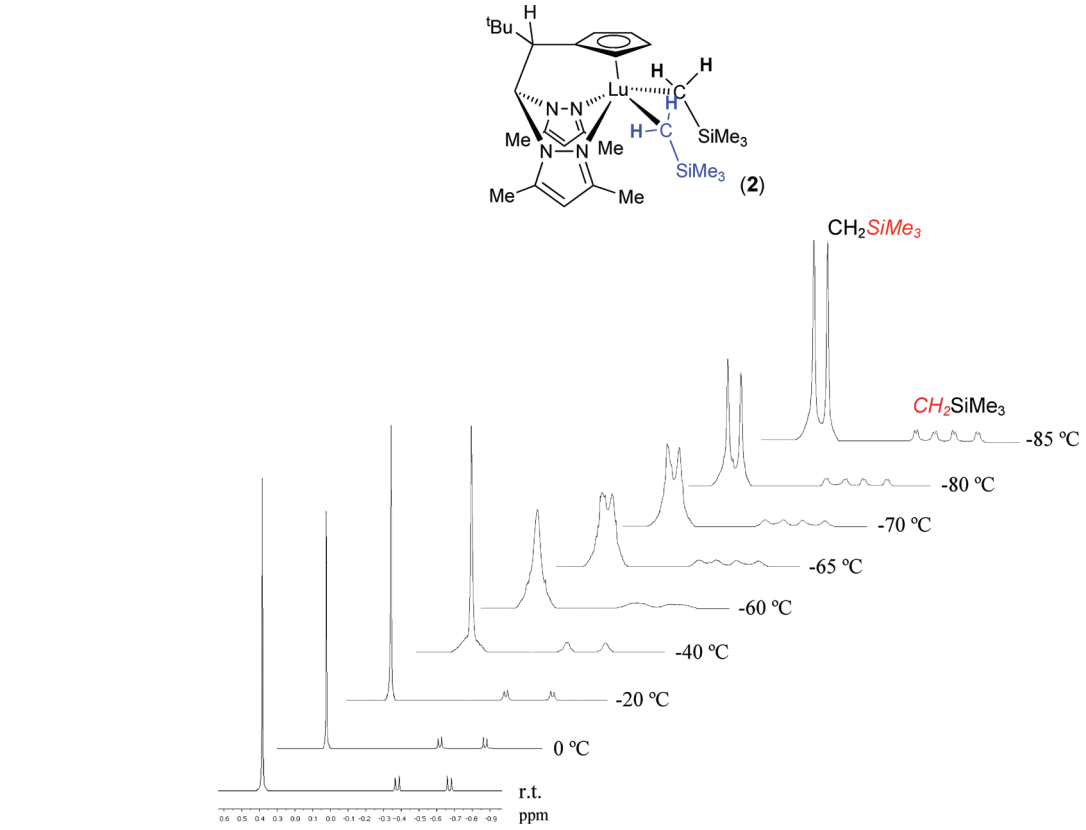

Figure 3. Variable-temperature ^{1}H NMR spectra in the region of the alkyl groups of complex **2**.

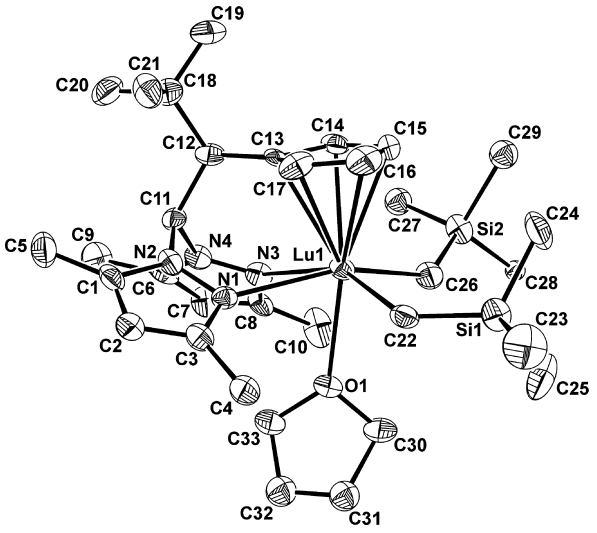

Figure 4. ORTEP view of **3**. Ellipsoids are at the 30% probability level, and hydrogen atoms have been omitted for clarity.

the expected *fac* coordination fashion. In addition, the lutetium center is coordinated to two trimethylsilylmethylene groups and one THF molecule, trans to the cyclopentadienyl ring. The geometry around the metal center is distorted octahedral, probably due to the constraints imposed by the chelating ligand. This substantial distortion is manifested in the angles N(3)−Lu(1)−N(1), C(22)−Lu(1)−N(3), and C(26)−Lu(1)−N(1), with values for these angles being 69.9(4), 152.7(5), and 157.4(4)°, respectively. The Lu−C bond lengths of 2.40(2) and 2.37(1) Å and Lu−N bond lengths of 2.60(1) and 2.58(1) Å fall within the normal range reported in the literature.[10,17] Supramolecular CH−π interactions (Table 3) between single molecules in crystals of complex **3** that enable stereochemical information to be mediated in three dimensions have been identified and explain the formation of a conglomerate among molecules. A self-assembly of the molecules in complex **3** gives rise to a chain formed along the *b* axis by CH−π interactions between a Me unit (C25−H25B) of one alkyl group and the pyrazole ring (pz2) of the other molecule (see red lines in Figure 5). The H25B−(centroid of pyrazole) distance has a value of 2.993 Å. The degree of displacement of H25B from the center of the pyrazole ring (D_{offset}) is 1.12 Å. The assembly of different chains takes place through another intermolecular CH−π interaction established between the C29−H29A methyl of the other alkyl group and the pyrazole ring (pz1) of the other molecule from a neighbor chain (see violet lines in Figure 5). The H29A−(centroid of pyrazole) distance has a value of 3.078 Å, and the degree of displacement of H29A from the center of the pyrazole ring (D_{offset}) is 1.18 Å. These interactions give rise to a sheet extended to the *c* axis (Figure 5). Self-assembly of the sheets extended to the *bc* plane along the *a* axis by CH−π interactions between a Me group (C28−H28C) of a alkyl group and the pyrazole ring of the other molecule from a neighboring sheet (see blue lines in Figure 6). The H28C−(centroid of pyrazole) distance has a value of 3.046 Å. The degree of displacement of H28C from the center of the pyrazole ring (D_{offset}) is 1.19 Å.

Catalytic Hydroamination Studies. Complexes **1**−**3** were tested for catalytic intramolecular hydroamination processes. They were active for the hydroamination/cyclization of various aminopentene derivatives (see Tables 4 and 5). The catalyst activity was monitored by ^{1}H NMR spectroscopy by loading a NMR tube with catalyst and substrate and heating the reaction

dx.doi.org/10.1021/om2011672 | *Organometallics* 2012, 31, 2244−2255

Table 1. Crystal Data and Structure Refinement Details for 3 and 13

	3	13
mol formula	$C_{33}H_{59}LuN_4OSi_2$	$C_{55}H_{65}LuN_6 \cdot 2.5(C_7H_8)$
formula wt	758.99	1215.44
temp (K)	230(2)	230(2)
wavelength (Å)	0.710 73	0.710 73
cryst syst	monoclinic	monoclinic
space group	$P2_1$	$P2_1/n$
a (Å)	9.9720(6)	15.199(2)
b (Å)	19.5503(10)	25.257(3)
c (Å)	10.5346(6)	15.904(2)
β (deg)	114.459(3)	94.575(7)
V (Å^3)	1869.5(2)	6086(1)
Z	2	4
calcd density (g/cm^3)	1.348	1.326
abs coeff (mm^{-1})	2.733	1.670
F(000)	784	2532
crystal size (mm^3)	0.19 × 0.16 × 0.09	0.19 × 0.18 × 0.09
index ranges	$-11 \le h \le 11$	$-18 \le h \le 17$
	$-22 \le k \le 23$	$-30 \le k \le 28$
	$-12 \le l \le 12$	$-18 \le l \le 16$
no. of rflns collected	12 069	49 098
no. of indep rflns	6353 (R(int) = 0.0481)	10 525 (R(int) = 0.1400)
no. of data/restraints/params	6353/14/382	10 525/0/568
goodness of fit on F^2	1.057	0.859
final R indices ($I > 2\sigma(I)$)	R1 = 0.0637	R1 = 0.0457
	wR2 = 0.1498	wR2 = 0.1228
absolute structure param	0.016(19)	
largest diff peak and hole, e/Å^3	2.509 and −1.564	0.762 and −0.703

Table 2. Bond Lengths (Å) and Angles (deg) for 3

Bond Lengths			
Lu(1)−Ct(1)[a]	2.351	Lu(1)−N(3)	2.58(1)
Lu(1)−O(1)	2.50(1)	Lu(1)−C(22)	2.40(2)
Lu(1)−N(1)	2.60(1)	Lu(1)−C(26)	2.37(1)
Bond Angles			
N(3)−Lu(1)−N(1)	69.9(4)	C(22)−Lu(1)−O(1)	82.3(5)
O(1)−Lu(1)−N(1)	76.8(4)	C(26)−Lu(1)−N(3)	94.0(5)
O(1)−Lu(1)−N(3)	73.0(3)	C(26)−Lu(1)−O(1)	83.4(5)
C(22)−Lu(1)−N(1)	93.8(4)	C(26)−Lu(1)−C(22)	94.3(5)

[a]Ct(1) is the centroid of Cp ring.

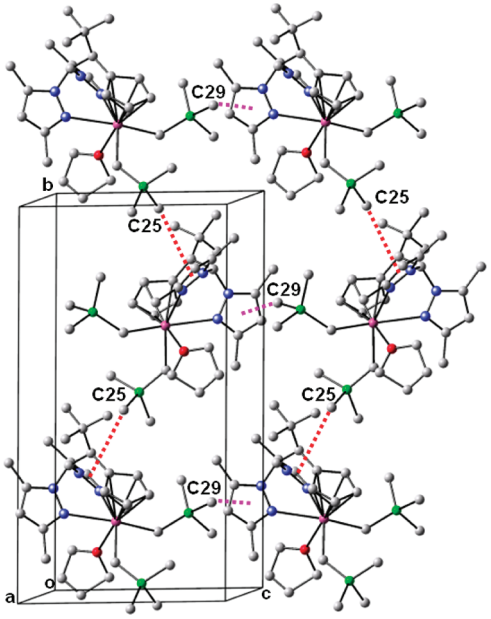

Figure 5. Ball-and-stick view of the intermolecular interactions in complex **3**. The CH−π interactions that give rise to chains are shown as red dashed lines, and the CH−π interactions that give rise to a sheet extended to the bc plane are shown as violet dashed lines. The hydrogen atoms are omitted for clarity.

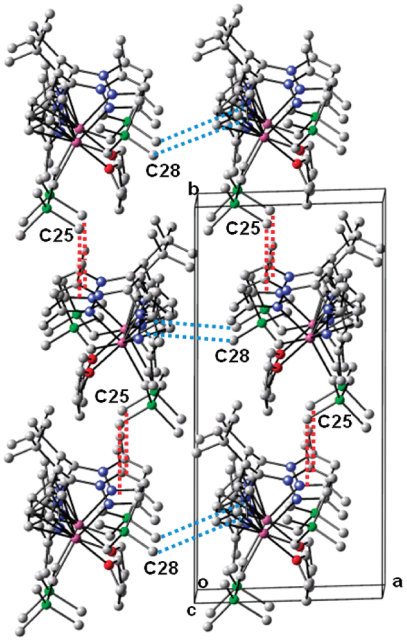

Figure 6. Self-assembly of the sheets extended to the bc plane along the a axis. The CH−π interactions that give rise to explain the conglomerate formation among molecules are shown as blue dashed lines.

mixtures to different temperatures. Initially, to test their reactivity the hydroamination of 2,2-diphenyl-4-pentenylamine (**4**) was performed.[18] The alkyl complexes **1**−**3** displayed high catalytic activity in the hydroamination/cyclization of aminopentene (**4**) to give the cyclic product **7** under mild conditions with a very low catalyst loading and short reaction times (Table 4). The catalytic activities of complexes **1**−**3** in the hydroamination of substrate **4** were lower in comparison to highly active lanthanocene catalysts and are more comparable to the activity found for other cyclopentadienyl and nonmetallocene lanthanide-based complexes.[4] Complex **3** promoted an

Table 3. CH−π Interactions for Complex 3 (Å, deg)

	d(H···cent)	d(C−H···cent)	d(H···atom)	α(C−Hcent)	d_{offset}	Figure 5 or 6 line color
H25B−pz2(N3N4)	2.993	3.819	2.782 (C6)	145.01	1.12	red
H29A−pz1(N1N2)	3.078	3.748	2.992 (C2)	128.16	1.18	violet
H28C−pz1(N1N2)	3.046	3.787	2.550 (C2)	135.14	1.19	blue

dx.doi.org/10.1021/om2011672 | *Organometallics* 2012, 31, 2244−2255

Table 4. Hydroamination/Cyclization Reactions of Aminoalkenes Catalyzed by Complexes 1−3

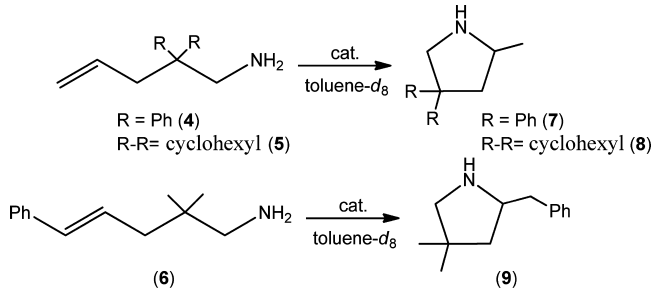

entry	cat.	substrate	[cat.]/[substrate] (%)	T (°C)	t (h)	yield (%)[a]	TOF (h^{-1})	ee (%)[b]
1	**1**	**4**	1	20	1.5	98	65.3	0
2	**1**	**4**	2	20	0.6	95	79.2	0
3	**1**	**4**	5	20	0.3	92	61.3	0
4	**1**	**4**	10	20	0.1	98	98.0	0
5	**1**	**5**	1	20	2.0	92	46.0	0
6	**1**	**5**	1	60	1.0	96	96.0	0
7	**1**	**5**	1	70	0.6	95	158.3	0
8	**1**	**5**	3	20	0.4	96	80.0	0
9	**1**	**6**	10	60	11.0	98	0.9	0
10	**1**	**6**	10	80	10.1	96	0.9	0
11	**1**	**6**	10	100	8.2	95	1.2	0
12	**2**	**4**	1	20	1.8	99	55.0	0
13	**2**	**4**	1	60	0.7	98	140.0	0
14	**2**	**4**	1	75	0.4	94	235.0	0
15	**2**	**4**	1	90	0.2	90	450.0	0
16	**2**	**5**	1	20	2.0	98	49.0	0
17	**2**	**5**	1	60	0.6	96	160.0	0
18	**2**	**5**	1	70	0.5	97	194.0	0
19	**2**	**5**	1	90	0.4	95	237.5	0
20	**2**	**6**	10	60	9.5	98	1.0	0
21	**2**	**6**	10	70	9.0	95	1.0	0
22	**2**	**6**	10	80	8.1	96	1.2	0
23	**3**	**4**	1	20	2.0	98	49.0	64
24	**3**	**4**	1	60	0.8	99	123.7	43
25	**3**	**4**	1	70	0.4	90	247.5	42
26	**3**	**4**	1	90	0.2	95	475.0	40
27	**3**	**4**	3	65	0.4	90	75.0	50
28	**3**	**4**	10	20	0.1	95	95.0	66
29	**3**	**5**	1	20	2.0	95	47.0	60
30	**3**	**5**	1	60	0.5	98	196.0	40
31	**3**	**5**	1	70	0.4	96	240.0	36
32	**3**	**5**	1	90	0.4	97	242.5	30
33	**3**	**5**	3	20	0.3	99	110.0	65
34	**3**	**6**	5	60	18.0	52	0.6	-
35	**3**	**6**	10	60	10.0	98	0.9	70
36	**3**	**6**	10	80	8.0	97	1.2	55

[a]NMR yield determined relative to ferrocene internal standard. [b]Enantiomeric excess determined by ^{19}F NMR of Mosher amides.

asymmetric cyclization of substrate **4** up to 66% ee (Table 4, entry 28). A decrease in the enantioselectivity values (Table 4, entries 23−26) with the temperature was observed. A positive effect of the temperature and catalyst loading on the catalyst activity was observed (Table 4).

In order to determine the scope of complexes **1−3** as precatalysts, a variety of aminoalkenes were tested at various reaction conditions. Entries 5−8, 16−19, and 29−33 (Table 4) correspond to the results obtained in the hydroamination/cyclization of (1-allylcyclohexyl)methylamine (**5**), bearing a cyclohexyl unit in the geminal position. For this substrate the catalyst activity is lower than for **4**, probably due to the significant Thorpe−Ingold effect of the geminal phenyl units in **4** (see, for example, at 90 °C a comparison of TOF values, entries 15 versus 19 and 26 versus 32). We have also considered the hydroamination/cyclization of an internal 1,2-disubstituted alkene, namely (*E*)-2,2-dimethyl-5-phenyl-4-penten-1-amine (**6**), to give the cyclic product **9** (Table 4, entries 9−11, 20−22, and 34−36). For this cyclization reaction much longer reaction times and higher catalyst loadings were required to get high yields. Complex **3** gives the cyclic product **9** up to 70% ee (Table 4, entry 35).

Quantitative kinetic studies of the hydroamination/cyclization of aminoalkene **4** by using **2** as catalyst were carried out,

dx.doi.org/10.1021/om2011672 | *Organometallics* 2012, 31, 2244−2255

Table 5. Hydroamination/Cyclization Reaction of 2-Allyl-2-methylpent-4-enylamine (10) Catalyzed by Complex 2

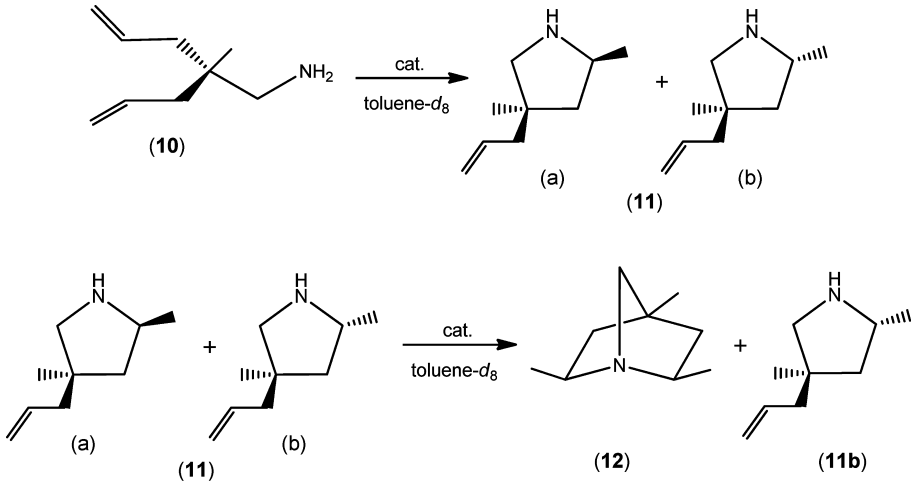

entry	cat.	substrate	product	[cat.]/[substrate] (%)	T (°C)	t (h)	yield (%)	TOF (h^{-1})	dr (a:b)
1	**2**	**10**	**11**	5	60	0.8	99[a]	24.7	1.2:1
2	**2**	**10**	**11**	5	100	0.4	98[a]	49.0	1.2:1
3	**2**	**11**	**12**	5	60	17.5	40[b] (98)[c]	0.5	exo,exo
4	**2**	**11**	**12**	5	100	9.1	41[b] (98)[c]	0.9	exo,exo

[a]NMR yield determined relative to ferrocene internal standard. [b]Isolated yield respect to compound **10**. [c]Percent conversion of diastereoisomer **11a**.

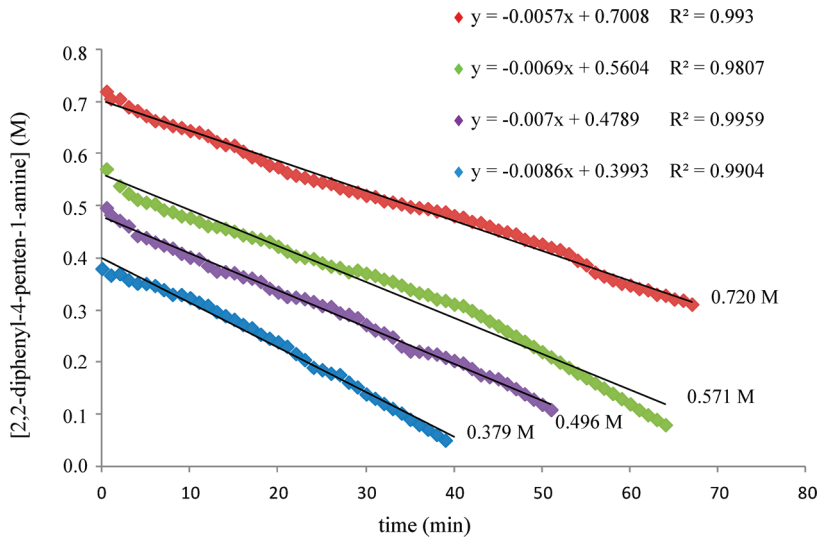

Figure 7. Linear regression fits for [2,2-diphenyl-4-penten-1-amine] versus time obtained for the first 30 min, indicating that the reactions are zero-order in substrate concentration. Plot of [2,2-diphenyl-4-penten-1-amine] versus time, illustrating zero-order dependence on [2,2-diphenyl-4-penten-1-amine]. The concentration of catalyst **2** is 0.024 M.

with the reaction monitored in situ by ^{1}H NMR spectroscopy (see the Supporting Information). Linear plots of substrate concentration versus time were obtained for runs in the range 0.38−0.72 M, with the precatalyst concentration kept constant, indicating that the reaction is zero order in substrate concentration (Figure 7). Furthermore, a linear response was observed for the reaction rate versus precatalyst concentration, with the initial substrate concentration kept constant (Figures 8 and 9), indicating that the reaction is first order in catalyst concentration. This empirical rate law is typical of lanthanide-mediated aminoalkene hydroamination/cyclization kinetics, which shows zero-order dependence on substrate concentration and first-order dependence on precatalyst concentration. The most fruitful comparison is with Marks' lanthanide systems, for which a wealth of mechanistic information is available and for which an imido mechanism is excluded.

Rare-earth catalysts, which catalyze the hydroamination reaction through a σ-bond insertion mechanism, can also react with secondary amine substrates. Thus, we explored the tandem cyclization reaction of the substrate 2-allyl-2-methylpent-4-enylamine (**10**) with compound **2** (Table 5). In the first step the allyl-substituted secondary amine **11** was formed, and this reacted further to give the tertiary amine **12**. Cyclization of **10** (Table 5, entries 1 and 2) proceeded in quantitative yield, and two diastereoisomers of pyrrolidine **11** were obtained (Figure S9, Supporting Information). The diastereoselectivity for **11** is low, and it is believed that the major isomer **11a** has the methyl group in the 2-position and the sterically slightly more demanding allyl substituent in the 4-position with a cis orientation relative to

dx.doi.org/10.1021/om2011672 | *Organometallics* 2012, 31, 2244−2255

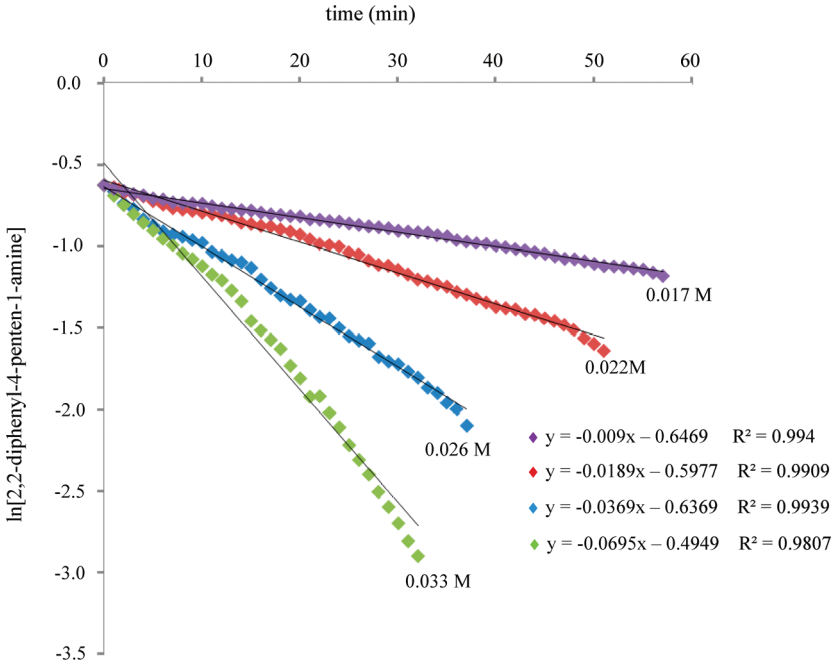

Figure 8. Linear regression fits for ln [2,2-diphenyl-4-penten-1-amine] versus time obtained for the first 30 min. Plot of ln [2,2-diphenyl-4-penten-1-amine] versus time for several catalyst **2** concentrations (0.017, 0.022, 0.026, 0.033 M). The concentration of 2-diphenyl-4-penten-1-amine is 0.534 M.

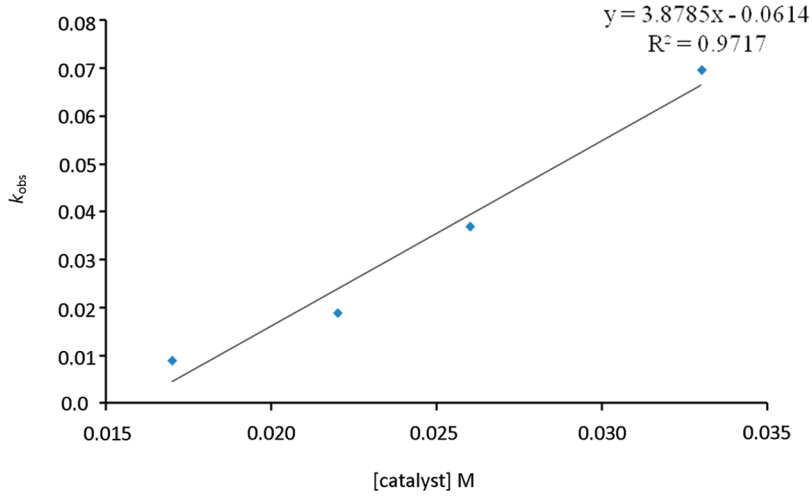

Figure 9. Plot of k_{obs} versus concentration of [Lu(CH_2SiMe_3)$_2$(bpztcp)] (**2**) for the cyclization of 2,2-diphenyl-4-penten-1-amine (**4**), showing first-order dependence on catalyst concentration.

each other.[19] This tandem cyclization reaction of **10** needed longer reaction times, yielding the tertiary amine **12** with 40% and 41% conversion (Table 5, entries 3 and 4, respectively). The tertiary amine **12** is isolated together with the minority isomer of the secondary amine **11b** (Figures S9 and S10, Supporting Information) but with high diastereoselectivity to the exo,exo product by preferential bicyclization of diastereoisomer **11a** from the secondary amine which has the methyl group in the 2-position and the allyl subtituent in the 4-position with cis orientation relative to each other.[19]

In order to gain an insight into the proposed general mechanism for rare-earth-metal-catalyzed hydroamination,[4,6] we decided to investigate the stoichiometric reaction of **2** with the substrate **4** on the NMR-tube scale using toluene-d_8 as solvent at room temperature. The progress of the reaction was monitored by NMR spectroscopy. The clean formation of the dipyrrolidinide–lutetium complex [Lu(NC_4H_5-2-Me-4,4-Ph_2)$_2$(bpztcp)] (**13**) (Scheme 3) was observed, and the product was unambiguously characterized spectroscopically.[5e] This dipyrrolidinide–lutetium complex **13** is also well observed when the catalytic cyclization reaction of substrate **4** with **2** as catalyst is carried out with higher catalyst loadings (see Figure S5b, Supporting Information). The formation of **13** is consistent with the mechanism proposed for the hydroamination/cyclization of aminoalkenes with our precatalysts (Figure 1). In fact, treatment of complex **2** with 2 equiv of **4** would lead to the transient bis-amido species **A** through a well-documented protonolysis process. This species could subsequently coordinate the pendant alkene to give the insertion step through the proposed four-membered transition states **B** and **B′**. However, in the absence of more substrate **4**, the proposed dialkyllutetium intermediate **C** would undergo an intramolecular

dx.doi.org/10.1021/om2011672 | *Organometallics* 2012, 31, 2244–2255

Scheme 3. Synthesis of Dipyrrolidinide Lutetium Complex 13 from the Stoichiometric Reaction of 2 with 4

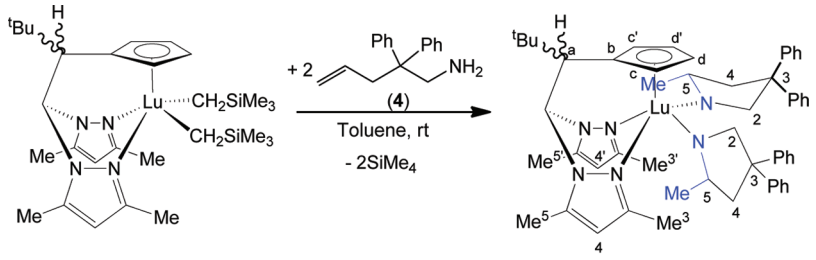

proton transfer to give the final product **13**. The NMR data corroborate the formation of the 5-exo regioisomer versus 6-endo, and this is consistent with the previously determined regioselectivity of the intramolecular hydroamination/cyclization of aminopentenes catalyzed by rare-earth catalysts.[4−6] When the reaction was carried out in a 1:1 (**2**:**4**) molar ratio, the dipyrrolidinide−lutetium complex [Lu(NC_4H_5-2-Me-4,4-Ph_2)$_2$(bpztcp)] (**13**) was formed together with the precursor complex [Lu(CH_2SiMe_3)$_2$(bpztcp)] (**2**). In the presence of an excess of substrate, intermolecular proton transfer would lead to the protonolysis of the proposed dialkyl−lutetium intermediate to regenerate the catalytically active species **A**.[20] Additionally, complex **13** exhibited catalytic activity in the hydroamination/cyclization process; thus, treatment of complex **13** with a large excess of substrate **4** at 70 °C led to complete conversion into the pyrrolidine **7** in less than 2 h. Attempts to isolate the proposed dialkyl−lutetium intermediate **C** were unsuccessful, even when the stoichiometric reaction of **2** with the substrate **4** was carried out at lower temperatures.

Complex **13** was also synthesized on the preparative scale and was isolated as pale yellow solid in good yield (90%) after the appropriate workup procedure (see the Experimental Section). Complex **13** has a chiral carbon in the heteroscorpionate scaffold and two chiral carbons in the N-heterocycles, a situation that could generate four diastereoisomers. However, the spectroscopic data of **13** show that there are only two diastereoisomers in solution (Figure S5a, Supporting Information). The molecular structure of complex **13** was confirmed by X-ray crystallographic analysis. The corresponding ORTEP drawing is depicted in Figure 10. Crystallographic data and selected interatomic distances and angles are given in Tables 1 and 6, respectively. The molecular structure determined by

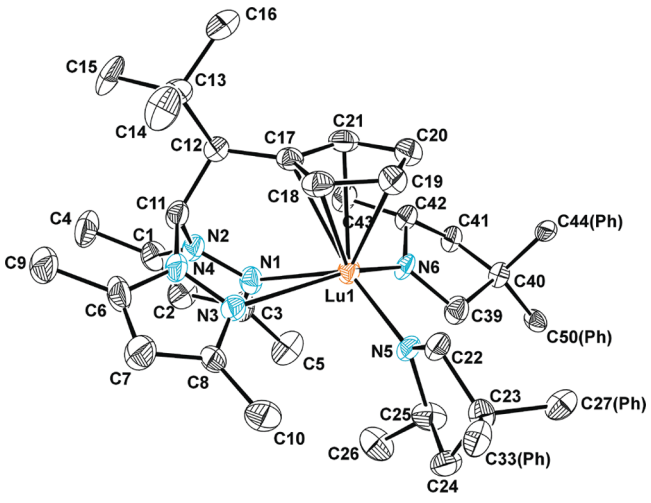

Figure 10. ORTEP representation of the molecular structure of **13** (ellipsoids drawn at 30% probability). H atoms and phenyl groups from N-bound heterocycles are omitted for clarity.

Table 6. Bond Lengths (Å) and Angles (deg) for 13

Bond Lengths			
Lu(1)−N(1)	2.485(8)	Lu(1)−N(6)	2.193(7)
Lu(1)−N(3)	2.710(8)	Lu(1)−Ct(1)[a]	2.336
Lu(1)−N(5)	2.167(7)		
Bond Angles			
N(5)−Lu(1)−N(6)	98.9(3)	N(6)−Lu(1)−N(3)	151.6(3)
N(5)−Lu(1)−N(1)	131.4(3)	N(1)−Lu(1)−N(3)	66.6(2)
N(6)−Lu(1)−N(1)	87.4(3)	C(22)−N(5)−C(25)	104.1(7)
N(5)−Lu(1)−N(3)	90.6(3)	C(42)−N(6)−C(39)	106.7(7)

[a]Ct(1) is the centroid of the Cp ring.

X-ray diffraction is in good agreement with the solution structure deduced from the NMR experiments. In the solid state, the crystal contains a racemic mixture of a single diastereoisomer (*RSS*/*SRR*), and the structure of the *SRR* enantiomer is depicted in Figure 10. The heteroscorpionate ligand is attached to the lutetium atom through the two nitrogen atoms of pyrazole rings and the cyclopentadienyl ring in a κ^2-NN-η^5-Cp coordination mode in the expected *fac* coordination fashion. In addition, the lutetium center is coordinated to two pyrrolidinide ligands. The coordination environment of the lutetium atom can be described as a distorted trigonal bipyramid, probably due to the steric demand of pyrrolidinide ligands and the constraints imposed by the chelating ligand. This substantial distortion is manifested in the angles N(1)−Lu(1)−N(3), N(6)−Lu(1)−N(3), and N(5)−Lu(1)−N(1), with values for these angles being 66.6(2), 151.6(3), and 131.4(3)°, respectively. The Lu(1)−N(3) bond length of 2.710(8) Å is longer than the Lu(1)−N(1) bond length of 2.485(8) Å due to the trans effect from pyrrolidinide ligand. The Lu−N5 and Lu−N6 bond lengths of 2.167(7) and 2.193(7) Å respectively confirm that the N atoms of the heterocyclic groups are attached to the lutetium center in an anionic fashion.[21] The structure of **13** also indicates that the two alkyl moieties of **2** are active sites for the catalyzed hydroamination/cyclization reaction, as proposed in Figure 1.

■ CONCLUSIONS

In conclusion, we report here a facile synthesis of a new family of dialkyl heteroscorpionate lutetium compounds bearing cyclopentadienyl groups as pendant donor arms. The lutetium complex **3** was isolated enantiomerically enriched by a spontaneous resolution of a racemic mixture and the preferential crystallization of one enantiomer due to the formation of a conglomerate among molecules. These lutetium complexes promoted efficiently the intramolecular hydroamination of

several aminopentenes. Complex **3** promoted the asymmetric hydroamination reaction of the aminopentenes, and up to 70% ee could be reached in the preparation of cyclic compound **9**. The dipyrrolidinide lutetium complex **13** has been isolated and characterized by a stoichiometric reaction of **2** with the substrate **4**. To the best of our knowledge, this complex represents the first example of an X-ray characterized dipyrrolidinide rare-earth-metal complex. Their formation is consistent with the general insertion mechanism for rare-earth metal catalysts, and it must evolve from a bis-alkyl key catalytic intermediate resulting from an insertion step of a C=C moiety into a metal–amido bond. Furthermore, this amido complex **13** is itself catalytically competent, as previously reported for other amido-containing group 3 and rare-earth-metal complexes. Further studies are being carried out to thoroughly examine the effect of changes both to the rare-earth-metal center and the scorpionate ligand framework on the catalytical activity of complexes in hydroamination processes.

EXPERIMENTAL SECTION

All manipulations were performed under nitrogen, using standard Schlenk techniques. Solvents were predried over sodium wire (toluene, *n*-hexane) and distilled under nitrogen from sodium (toluene) or sodium–potassium alloy (*n*-hexane). Deuterated solvents were stored over activated 4 Å molecular sieves and degassed by several freeze–thaw cycles. Microanalyses were carried out with a Perkin-Elmer 2400 CHN analyzer. ^{1}H, ^{13}C, and ^{19}F NMR spectra were recorded on a Varian Innova FT-500 (^{1}H NMR 500 MHz, ^{13}C NMR 125 MHz, and ^{19}F NMR 470 MHz) spectrometer and referenced to the residual deuterated solvent. The NOESY-1D spectra were recorded with the following acquisition parameters: irradiation time 2 s and number of scans 256, using standard VARIANT-FT software. Two-dimensional NMR spectra were acquired using standard VARIANT-FT software and processed using an IPC-Sun computer. The specific rotation $[\alpha]_D^{22}$ was measured at 22 °C on a Perkin-Elmer 241 polarimeter equipped with a Na lamp operating at 589 nm with a light path length of 10 cm. $LuCl_3$ was used as purchased (Aldrich), and $[LuCl_3(thf)_3]$,[22] $[Lu(CH_2SiMe_3)_3(thf)_2]$,[12] bpzcpH,[10d] bpztcpH,[10d] 2,2-diphenyl-4-penten-1-amine (**4**),[23] (1-allylcyclohexyl)methylamine (**5**),[23] (*E*)-2,2-dimethyl-5-phenyl-4-penten-1-amine (**6**),[23] and 2-allyl-2-methyl-4-penten-1-amine (**10**)[23] were prepared according to literature procedures.

Synthesis of [Lu(CH$_2$SiMe$_3$)$_2$(bpzcp)] (1). A solution of bpzcpH (0.30 g, 0.69 mmol) in toluene (20 mL) was added dropwise to a cooled (0 °C) solution of $[Lu(CH_2SiMe_3)_3(thf)_2]$ (0.40 g, 0.69 mmol) in toluene (20 mL). The reaction mixture was stirred for 2 h at 0 °C. Evaporation of the solvent gave a white solid. The solid was recrystallized from toluene/hexane (10/1, 20 mL at −20 °C) to give colorless crystals of the compound **1**. Yield: 0.40 g (75%). Anal. Calcd for $C_{37}H_{51}LuN_4Si_2$: C, 56.8; H, 6.6; N, 7.2. Found: C, 56.9; H, 7.0; N, 7.0. ^{1}H NMR (C_6D_6, 297 K): δ 6.93 (s, 1 H, CH), 5.25 (s, 2 H, H^4), 2.42 (s, 6 H, Me^3), 1.34 (s, 6 H, Me^5), 7.42–6.90 (m, 10 H, Ph), 6.73 (m, 2 H, H^d-Cp), 5.70 (m, 2 H, H^c-Cp), 0.47 (s, 18 H, $LuCH_2SiMe_3$), −0.49 (s, 4 H, $LuCH_2SiMe_3$). ^{13}C{^{1}H} NMR (C_6D_6, 297 K): δ 75.2 (CH), 145.3, 142.1 (C$^{3\text{ or }5}$), 108.3 (C$^{4\prime}$), 15.6 (Me^3), 11.4 (Me^5), 151.7–128.3 (Ph), 61.0 (C^a), 110.0 (C^b-Cp), 118.1 (C^c-Cp), 110.7 (C^d-Cp), 38.7 ($LuCH_2SiMe_3$), 5.1 ($LuCH_2SiMe_3$).

Synthesis of [Lu(CH$_2$SiMe$_3$)$_2$(bpztcp)] (2). The synthetic procedure was the same as for complex **1**, using bpztcpH (0.23 g, 0.69 mmol), $[Lu(CH_2SiMe_3)_3(thf)_2]$ (0.40 g, 0.69 mmol), and toluene (20 mL) to give **2** as a white solid. Yield: 0.38 g (80%). Anal. Calcd for $C_{29}H_{51}LuN_4Si_2$: C, 50.7; H, 7.5; N, 8.2. Found: C, 50.9; H, 7.6; N, 8.5. ^{1}H NMR (C_6D_6, 297 K): δ 6.25 (s, 1 H, CH), 5.26 (s, 1 H, H^4), 5.24 (s, 1 H, H$^{4\prime}$), 2.45 (s, 3 H, Me^3), 2.30 (s, 3 H, Me $^{3\prime}$), 1.75 (s, 3 H, Me^5), 1.61 (s, 3 H, Me$^{5\prime}$), 2.60 (s, 1 H, CH^a), 0.78 (s, 9 H, $C(CH_3)_3$), 6.75, 6.71 (m, 2 H, H$^{d,d\prime}$-Cp), 6.18, 5.58 (m, 2 H, H$^{c,c\prime}$-Cp), 0.50 (s, 18 H, $LuCH_2SiMe_3$), A −0.33, B −0.59 (AB, J_{AB} = 11.2 Hz, 4 H, $LuCH_2SiMe_3$). ^{13}C{^{1}H} NMR (C_6D_6, 297 K): δ 67.1 (CH), 152.4, 150.9, 140.2, 139.6 (C$^{3,3\prime\text{ or }5,5\prime}$), 108.2, 107.5 (C$^{4,4\prime}$), 15.7 (Me^3), 15.4 (Me$^{3\prime}$), 11.9 (Me$^{5\prime}$), 10.9 (Me^5), 57.8 (C^a), 35.2 ($C(CH_3)_3$)), 28.4 ($C(CH_3)_3$), 110.6 (C^b-Cp), 116.4 (C^c-Cp), 114.2 (C$^{c\prime}$-Cp), 110.9, (C$^{d\prime}$-Cp), 109.9 (C^d-Cp), 37.2, 35.0 ($LuCH_2SiMe_3$), 5.0 ($LuCH_2SiMe_3$).

Synthesis of [Lu(CH$_2$SiMe$_3$)$_2$(bpztcp)(thf)] (3). A solution of bpzctpH (0.23 g, 0.69 mmol) in toluene (5 mL) was added dropwise to a cooled (0 °C) solution of $[Lu(CH_2SiMe_3)_3(thf)_2]$ (0.40 g, 0.69 mmol) in hexane (10 mL). The reaction mixture was stored without stirring at −20 °C for 48 h. Colorless crystals of the highly enantiopure complex **3** were obtained. Yield: 0.18 g (35%). $[\alpha]_D^{25}$ = −21.3° (*c* 0.10, toluene). Anal. Calcd for $C_{33}H_{59}LuN_4OSi_2$: C, 52.2; H, 7.8; N, 7.4. Found: C, 52.0; H, 7.8; N, 7.5. ^{1}H NMR (C_6D_6, 297 K): δ 6.26 (s, 1 H, CH), 5.30 (s, 1 H, H^4), 5.27 (s, 1 H, H$^{4\prime}$), 2.39 (s, 3 H, Me^3), 2.25 (s, 3 H, Me $^{3\prime}$), 1.81 (s, 3 H, Me^5), 1.65 (s, 3 H, Me$^{5\prime}$), 2.60 (s, 1 H, CH^a), 0.80 (s, 9 H, $C(CH_3)_3$), 6.71, 6.69 (m, 2 H, H$^{d,d\prime}$-Cp), 6.12, 5.40 (m, 2 H, H$^{c,c\prime}$-Cp), 0.42 (s, 18 H, $LuCH_2SiMe_3$), A −0.41, B −0.69 (AB, J_{AB} = 11.2 Hz, 4 H, $LuCH_2SiMe_3$), 3.51 (m, 4 H, THF), 1.43 (m, 4 H, THF). ^{13}C{^{1}H} NMR (C_6D_6, 297 K): δ 67.6 (CH), 152.0, 151.0, 140.6, 139.5 (C$^{3,3\prime\text{ or }5,5\prime}$), 108.7, 108.0 (C$^{4,4\prime}$), 15.9 (Me^3), 15.5 (Me$^{3\prime}$), 12.1 (Me$^{5\prime}$), 11.1 (Me^5), 57.6 (C^a), 35.7 ($C(CH_3)_3$), 28.6 ($C(CH_3)_3$), 110.0 (C^b-Cp), 116.7 (C^c-Cp), 114.6 (C$^{c\prime}$-Cp), 111.3, (C$^{d\prime}$-Cp), 109.7 (C^d-Cp), 36.2, 35.5 ($LuCH_2SiMe_3$), 5.2 ($LuCH_2SiMe_3$), 68.1 (THF), 25.4 (THF).

Synthesis of [Lu(NC$_4$H$_5$-2-Me-4,4-Ph$_2$)$_2$(bpztcp)] (13). A solution of 1-amino-2,2-diphenyl-4-pentene (**4**; 0.15 g, 0.64 mmol) in toluene (20 mL) was added to a solution of $[Lu(CH_2SiMe_3)_2$(bpztcp)] (**2**; 0.22 g, 0.32 mmol) in toluene (20 mL). The reaction mixture was stirred for 1 h at room temperature. The solvent was removed under vacuum and the remaining residue washed with hexane (20 mL) to yield compound **13** as a pale yellow solid. The solid was recrystallized from toluene/hexane (10/1, 20 mL at −20 °C) to give pale yellow crystals of the compound **13**. Yield: 0.52 g (90%). Anal. Calcd for $C_{55}H_{65}LuN_6$: C, 67.0; H, 6.6; N, 8.5. Found: C, 67.1; H, 6.9; N, 8.3. ^{1}H NMR (C_6D_6, 297 K; two diastereoisomers): δ 6.30, 6.24 (s, 2 H, CH), 5.31, 5.27, 5.25, 5.20 (s, 4 H, H^4, H$^{4\prime}$), 2.72, 2.51, 2.37, 2.31 (s, 12 H, Me$^{3,3\prime}$), 1.73, 1.64, 1.60, 1.56 (s, 12 H, Me$^{5,5\prime}$), 2.78 (s, 2 H, CH^a), 0.79, 0.77 (s, 18 H, $C(CH_3)_3$), 6.95, 6.66, 6.44, 6.21, 6.11, 6.06, 5.70, 5.57 (m, 8 H, Cp), 8.15–6.98 (m, 40 H, *Ph* NCHMeCH$_2$ C*Ph*$_2$CH$_2$), 4.40–4.10 (m, 12 H, *H*^{5} and *H*^{2} NC*H*MeCH$_2$CPh$_2$C*H*$_2$), 2.41, 1.75 (m, 8 H, *H*^{4} NCHMeC*H*$_2$CPh$_2$CH$_2$), 1.47, 1.13 (m, 12 H, *Me*^{5} NCH*Me*CH$_2$CPh$_2$CH$_2$). ^{13}C{^{1}H} NMR (C_6D_6, 297 K; two diastereoisomers): δ 66.5 (CH), 154.4, 148.7, 148.1, 139.3, 139.0, 137.7 (C$^{3,3\prime\text{ or }5,5\prime}$), 107.5, 107.3, 107.2, 107.1 (C$^{4,4\prime}$), 15.9, 15.6, 14.0, 12.9 (Me$^{3,3\prime}$), 12.1, 11.8, 11.7, 11.2, 11.1 (Me$^{5,5\prime}$), 58.7, 58.3 (C^a), 35.4, 35.2 ($C(CH_3)_3$), 28.4 ($C(CH_3)_3$), 125.3, 125.2, 114.7, 114.6, 114.2, 110.9, 110.8, 110.7, 110.2, 109.2 (Cp), 151.6, 151.4, 151.3, 151.2, 150.7, 150.6, 150.5, 150.3 (*^{i}C-Ph* NCHMeCH$_2$C*Ph*$_2$CH$_2$), 129.3, 129.1, 128.6. 128.5, 128.4, 128.3, 128.1, (*^{o}C-Ph* NCHMeCH$_2$ C*Ph*$_2$CH$_2$), 127.9, 127.8, 127.6, 127.5, 126.1, 126.0, 125.6, 125.4, 125.3 (*^{m}C-* and *^{p}C-Ph* NCHMeCH$_2$C*Ph*$_2$CH$_2$), 69.5, 66.6, 65.3 (NCHMeCH$_2$CPh$_2$CH$_2$), 59.9, 59.4, 58.7, 58.4 (NCHMeCH$_2$CPh$_2$ CH$_2$), 58.8, 58.6, 58.5 (NCHMeCH$_2$CPh$_2$CH$_2$), 51.3, 49.8, 49.5, 47.5 (NCHMeCH$_2$CPh$_2$CH$_2$), 25.6, 24.4, 22.4 (NCH*Me*CH$_2$CPh$_2$CH$_2$).

General Procedure for Catalytic Intramolecular Hydroamination. In a typical small-scale experiment, 0.01 mmol (0.0068 g) of catalyst $[Lu(CH_2SiMe_3)_2$(bpztcp)] (**2**) and 1.00 mmol (0.2377 g) of aminoalkene 2,2-diphenyl-4-penten-1-amine (**4**)[23] were dissolved in 0.75 mL of toluene-d_8 and placed in a J. Young style NMR tube with a resealable Teflon valve. The tube was closed and placed into an oil bath that was preheated at the temperature desired. The reaction was monitored at regular intervals by ^{1}H NMR spectroscopy to determine the optimum conversion.

X-ray Crystallographic Structure Determination. For X-ray structure analyses the crystals of compounds **3** and **13**·2.5C_7H_8 were mounted on a glass fibers with Paratone-N oil and transferred to a Bruker X8 APEX II CCD diffractometer using graphite-monochromated Mo Kα radiation (λ = 0.710 73 Å). Data were integrated and corrected for Lorentz–polarization effects using SAINT[24] and were

dx.doi.org/10.1021/om2011672 | *Organometallics* 2012, 31, 2244–2255

corrected for absorption effects using SADABS.[25] Space group assignments were based upon systematic absences, E statistics, and successful refinement of the structures. Structures were solved by direct methods with the aid of successive difference Fourier maps and were refined against all data using the SHELXTL software package.[26]

In the case of **3** one $SiMe_3$ and coordinated THF are disordered. The groups were modeled over two static sites, and the occupancies of the disorder components were refined initially and then fixed to a value of 50:50. Least-squares restraints have been used to obtain a better model. For **13**, the compound crystallizes with 2.5 disordered toluene molecules per asymmetric unit. The option squeeze[27] was used to eliminate the contribution of the electron density from the intensity data. The derived quantities M_r, $F(000)$, and D_x in the crystal data were corrected with the contribution from this disordered solvent. For both compounds, thermal parameters for all non-hydrogen atoms were refined anisotropically, with the exception of the atoms of disordered groups, which were assigned isotropic parameters due to a convergence to NPD anisotropic parameters for some atoms. Hydrogen atoms, added here, were assigned to ideal positions and refined using a riding model with an isotropic thermal parameter.

■ ASSOCIATED CONTENT

Supporting Information

Figures, text, tables, and CIF files giving experimental details, procedures for catalytic intramolecular hydroamination, kinetic measurements and representative kinetic plots, and X-ray crystallographic data for complexes **3** and **13**. This material is available free of charge via the Internet at http://pubs.acs.org.

■ AUTHOR INFORMATION

Corresponding Author

*E-mail: Antonio.Otero@uclm.es (A.O.). Tel: +34926295300. Fax: +34926295318.

Notes

The authors declare no competing financial interest.

■ ACKNOWLEDGMENTS

We gratefully acknowledge financial support from the Ministerio de Ciencia e Innovación (MICINN) of Spain (Grant Nos. CTQ2008-00318/BQU and Consolider-Ingenio 2010 ORFEO CSD2007-00006) and the Junta de Comunidades de Castilla-La Mancha, Spain (Grant No. PCI08-0010).

■ REFERENCES

(1) (a) Müller, T. E.; Hultzsch, K. C.; Yus, M.; Foubelo, F.; Tada, M. *Chem. Rev.* **2008**, *108*, 3795−3892. (b) Hultzsch, K. C. *Adv. Synth. Catal.* **2005**, *347*, 367−391. (c) Beller, M.; Seayad, J.; Tillack, A.; Jiao, H. *Angew. Chem., Int. Ed.* **2004**, *43*, 3368−3398. (d) Pohlki, F.; Doye, S. *Chem. Soc. Rev.* **2003**, *32*, 104−114. (e) Bytschkov, I.; Doye, S. *Eur. J. Org. Chem.* **2003**, *6*, 935−946. (f) Hartwig, J. F. *Science* **2002**, *297*, 1653−1654. (g) Brunet, J. J.; Neibecker, D. In *Catalytic Heterofunctionalization*; Togni, A., Gruetzmacher, H., Eds.; Wiley-VCH: Weinheim, Germany, 2001; pp 91−141.

(2) (a) Jiang, T.; Livinghouse, T. *Org. Lett.* **2010**, *12*, 4271−4273. (b) Zhang, W.; Werness, J. B.; Tang, W. *Org. Lett.* **2008**, *10*, 2023−2026. (c) Sakai, N.; Ridder, A.; Hartwig, J. F. *J. Am. Chem. Soc.* **2006**, *128*, 8134−8135. (d) Kumar, K.; Michalik, D.; Castro, I. G.; Tillack, A.; Zapf, A.; Arlt, M.; Heinrich, T.; Böttcher, H.; Beller, M. *Chem. Eur. J.* **2004**, *10*, 746−757. (e) Hartung, C. G.; Breindl., C.; Tillack, A.; Beller, M. *Tetrahedron* **2000**, *56*, 5157−5162. (f) Arredondo, V. M.; Tian, S.; McDonald, F. E.; Marks, T. J. *J. Am. Chem. Soc.* **1999**, *121*, 3633−3639.

(3) See for recent examples: (a) Taylor, J. G.; Adrio, L. A.; Hii, K. K. *Dalton Trans.* **2010**, *39*, 1171−1175. (b) Hesp, K. D.; Tobisch, S.; Stradiotto, M. *J. Am. Chem. Soc.* **2010**, *132*, 413−426. (c) Dub, P. A.; Rodríguez-Zubiri, M.; Daran, J.-C.; Brunet, J.-J.; Poli, R. *Organometallics* **2009**, *28*, 4764−4777. (d) Reznichenko, A. L.; Hampel, F.; Hultzsch, K. C. *Chem. Eur. J.* **2009**, *15*, 12819−12827. (e) McBee, J. L.; Bell, A. T.; Tilley, T. D. *J. Am. Chem. Soc.* **2008**, *130*, 16562−16571. (f) Kovács, G.; Ujaque, G.; Lledós, A. *J. Am. Chem. Soc.* **2008**, *130*, 853−864.

(4) See for example: (a) Manna, K.; Ellern, A.; Sadow, A. D. *Chem. Commun.* **2010**, *46*, 339−341. (b) Dunne, J. F.; Fulton, D. B.; Ellern, A.; Sadow, A. D. *J. Am. Chem. Soc.* **2010**, *132*, 17680−17683. (c) Leitch, D. C.; Payne, P. R.; Dunbar, C. R.; Schafer, L. L. *J. Am. Chem. Soc.* **2009**, *131*, 18246−18247. (d) Stubber, B. D.; Marks, T. J. *J. Am. Chem. Soc.* **2007**, *129*, 6149−6167. (e) Gribkov, D. V.; Hultzsch, K. C. *Angew. Chem., Int. Ed.* **2004**, *43*, 5542−5546. (f) Ryu, J.-S.; Li, Y.; Marks, T. J. *J. Am. Chem. Soc.* **2003**, *125*, 12584−12605. (g) Straub, B. F.; Bergman, R. G. *Angew. Chem., Int. Ed.* **2001**, *40*, 4632−4635. (h) Pohlki, F.; Doye, S. *Angew. Chem., Int. Ed.* **2001**, *40*, 2305−2308. (i) Gagné, M. R.; Stern, C. L.; Marks, T. J. *J. Am. Chem. Soc.* **1992**, *114*, 275−294.

(5) See for example: (a) Selby, J. D.; Schulten, C.; Schwarz, A. D.; Stasch, A.; Clot, E.; Jones, C.; Mountford, P. *Chem. Commun.* **2008**, 5101−5103. (b) Wood, M. C.; Leitch, D. C.; Yeung, C. S.; Kozak, J. A.; Schafer, L. L. *Angew. Chem., Int. Ed.* **2007**, *46*, 354−358. (c) Zhang, Z.; Leitch, D. C.; Lu, M.; Patrick, B. O.; Schafer, L. L. *Chem. Eur. J.* **2007**, *13*, 2012−2022. (d) Ward, B. D.; Maisse-Francois, A.; Mountford, P.; Gade, L. H. *Chem. Commun.* **2004**, 704−705. (e) Lauterwasser, F.; Hayes, P. G.; Bräse, S.; Piers, W. E.; Schafer, L. L. *Organometallics* **2004**, *23*, 2234−2237.

(6) (a) Hong, S.; Marks, T. J. *Acc. Chem. Res.* **2004**, *37*, 673−686. (b) Gagné, M. R.; Marks, T. J. *J. Am. Chem. Soc.* **1989**, *111*, 4108−4109.

(7) See for recent examples: (a) Benndorf, P.; Jenter, J.; Zielke, L.; Roesky., P. W. *Chem. Commun.* **2011**, *47*, 2574−2576. (b) Leitch, D. C.; Turner, C. S.; Schafer, L. L. *Angew. Chem., Int. Ed.* **2010**, *49*, 6382−6386. (c) Le Roux, E.; Liang, Y.; Storz, M. P.; Anwander, R. *J. Am. Chem. Soc.* **2010**, *132*, 16368−16371. (d) Aillaud, I.; Lyubov, D.; Collin, J.; Guillot, R.; Hannedouche, J.; Schulz, E.; Trifonov, A. *Organometallics* **2008**, *27*, 5929−5936.

(8) See for example: (a) Trofimenko, S. *Scorpionates: The Coordination Chemistry of Polypyrazolylborate Ligands*; Imperial College Press: London, 1998. (b) Pettinari, C. *Scorpionates II: Chelating Borate Ligands*; Imperial College Press: London, 2008. (c) Pettinari, C.; Pettinari, R. *Coord. Chem. Rev.* **2005**, *249*, 663−691. (d) Bigmore, H. R.; Lawrence, S. C.; Mountford, P.; Tredget, C. S. *Dalton Trans.* **2005**, 635−651. (e) Otero, A.; Fernández-Baeza, J.; Antiñolo, A.; Tejeda, J.; Lara-Sánchez, A. *Dalton Trans.* **2004**, 1499−1510. (f) Marques, N.; Sella, A.; Takats, J. *Chem. Rev.* **2002**, *102*, 2137−2160.

(9) See for example: (a) Santillan, G. A.; Carrano, C. J. *Dalton Trans.* **2009**, 6599−6605. (b) Godau, T.; Platzmann, F.; Heinemann, F. W.; Burzlaff, N. *Dalton Trans.* **2009**, 254−255. (c) Fischer, N. V.; Heinemann, F. W.; Burzlaff, N. *Eur. J. Inorg. Chem.* **2009**, 3960−3965. (d) Otero, A.; Fernández-Baeza, J.; Tejeda, J.; Lara-Sánchez, A.; Sánchez-Molina, M.; Franco, S.; López-Solera, I.; Rodríguez, A. M.; Sánchez-Barba, L. F.; Morante-Zarco, S.; Garcés, A. *Inorg. Chem.* **2009**, *48*, 5540−5554. (e) Howe, R. G.; Tredget, C. S.; Lawrence, S. C.; Subongkoj, S.; Cowley, A. R.; Mountford, P. *Chem. Commun.* **2006**, 223−225. (f) Otero, A.; Fernández-Baeza, J.; Antiñolo, A.; Tejeda, J.; Lara-Sánchez, A.; Sánchez-Barba, L.; Fernández-López, M.; López-Solera, I. *Inorg. Chem.* **2004**, *43*, 1350−1358.

(10) See for example: (a) Neal, S. R.; Ellern, A.; Sadow, A. D. *J. Organomet. Chem.* **2011**, *696*, 228−234. (b) Pawlikowski, A. V.; Ellern, A.; Sadow, A. D. *Inorg. Chem.* **2009**, *48*, 8020−8029. (c) Kopf, H.; Holzberger, B.; Pietraszuk, C.; Hübner, E.; Burzlaff, N. *Organometallics* **2008**, *27*, 5894−5905. (d) Otero, A.; Fernández-Baeza, J.; Antiñolo, A.; Lara-Sánchez, A.; Tejeda, J.; Sánchez-Barba, L.; Martínez-Caballero, E.; López-Solera, I. *Organometallics* **2008**, *27*, 976−983. (e) Cuomo, C.; Milione, S.; Grassi, A. *Macromol. Rapid Commun.* **2006**, *27*, 611−618. (f) Bigmore, H. R.; Lawrence, S. C.; Mountford, P.; Tredget, C. S. *Dalton Trans.* **2005**, 635−651. (g) Milione, S.; Bertolasi, V.; Cuenca, T.; Grassi, A. *Organometallics* **2005**, *24*, 4915−

4925. (h) Lawrence, S. C.; Ward, B. D.; Dubberley, S. R.; Kozak, C. M.; Mountford, P. *Chem. Commun.* **2003**, 1176−1177. (i) Milione, S.; Montefusco, C.; Cuenca, T.; Grassi, A. *Chem. Commun.* **2003**, 1176−1177. (j) Otero, A.; Fernández-Baeza, J.; Antiñolo, A.; Carrillo-Hermosilla, F.; Tejeda, J.; Diez-Barra, E.; Lara-Sánchez, A.; Sánchez-Barba, L.; López-Solera, I. *Organometallics* **2001**, *20*, 2428−2430.

(11) See for example: (a) Otero, A.; Fernández-Baeza, J.; Antiñolo, A.; Tejeda, J.; Lara-Sánchez, A.; Sánchez-Barba, L.; López-Solera, I.; Rodríguez, A. M. *Inorg. Chem.* **2007**, *46*, 1760−1770. (b) Adhikari, D.; Zhao, G.; Basuli, F.; Tomaszewski, J.; Huffman, J. C.; Mindiola, D. J. *Inorg. Chem.* **2006**, *45*, 1604−1610. (c) Kopf, H.; Pietraszuk, C.; Hübner, E.; Burzlaff, N. *Organometallics* **2006**, *25*, 2533−2546. (d) Hammes, B. S.; Chohan, B. S.; Hoffman, J. T.; Einwächter, S.; Carrano, C. J. *Inorg. Chem.* **2004**, *43*, 7800−7806. (e) Otero, A.; Fernández-Baeza, J.; Antiñolo, A.; Tejeda, J.; Lara-Sánchez, A.; Sánchez-Barba, L.; Rodríguez, A. M.; Maestro, M. A. *J. Am. Chem. Soc.* **2004**, *126*, 1330−1331. (f) Smith, J. N.; Shirin, Z.; Carrano, C. J. *J. Am. Chem. Soc.* **2003**, *125*, 868−869.

(12) (a) Arndt, S.; Spaniol, T. P.; Okuda, J. *Chem. Commun.* **2002**, 896−897. (b) Atwood, J. L.; Hunter, W. E.; Rogers, R. D.; Holton, J.; McMeeking, J.; Pearce, R.; Lappert, M. F. *J. Chem. Soc., Chem. Commun.* **1978**, 140−142. (c) Lappert, M. F.; Pearce, R. *J. Chem. Soc., Chem. Commun.* **1973**, 126−126.

(13) (a) Hamelin, O.; Pecaut, J.; Fontecave, M. *Chem. Eur. J.* **2004**, *10*, 2548−2555. (b) Lennartson, A.; Vestergren, M.; Håkansson, M. *Chem. Eur. J.* **2005**, *11*, 1757−1762. (c) Ou, G.-C.; Jiang, L.; Feng, X.-L.; Lu, T.-B. *Inorg. Chem.* **2008**, *47*, 2710−2718. (d) Gil-Hernandez, B.; Höppe, H. A.; Vieth, J. K.; Sanchiz, J.; Janiak, C. *Chem. Commun.* **2010**, *46*, 8270−8272. (e) Lennartson, A.; Olsson, S.; Sundberg, J.; Håkansson, M. *Angew. Chem., Int. Ed.* **2009**, *48*, 3137−3140. (f) Pettersen, A.; Lennartson, A.; Håkansson, M. *Organometallics* **2009**, *28*, 3567−3569. (g) Jacques, J.; Collet, A.; Wilen, S. H. *Enantiomers, Racemates and Resolutions*; Wiley: New York, 1984.

(14) Perez-García, L.; Amabilino, D. B. *Chem. Soc. Rev.* **2002**, *31*, 342−356.

(15) (a) Jacques, J.; Collet, A.; Wilen, S. H. *Enantiomers, Racemates and Resolutions*, Krieger Publishing: Malaber, FL, 1994. (b) Pratt-Brock, C.; Dunitz, J. D. *Chem. Mater.* **1994**, *6*, 1118−1127. (c) Kostyanovsky, R. G.; Avdeenko, A. P.; Konovalova, S. A.; Kadorkina, G. K.; Prosyanick, A. V. *Mendeleev Commun.* **2000**, 16−19. (d) Johansson, A.; Håkansson, M. *Chem. Eur. J.* **2005**, *11*, 5238−5248.

(16) Sandström, J. *Dynamic NMR Spectroscopy*; Academic Press: New York, 1982.

(17) Zhang, Z.; Cui, D.; Trifonov, A. A. *Eur. J. Inorg. Chem.* **2010**, 2861−2866.

(18) Hong, S. W.; Tian, S.; Metz, M. V.; Marks, T. J. *J. Am. Chem. Soc.* **2003**, *125*, 14768−14783.

(19) (a) Stanlake, L. J. E.; Schafer, L. L. *Organometallics* **2009**, *28*, 3990−3998. (b) Hultzsch, K. C.; Hampel, K. C.; Wagner, T. *Organometallics* **2004**, *23*, 2601−2612.

(20) It is noteworthy that some studies suggest that the insertion and protonolysis step may be concerted. See for example: (a) Arrowsmith, M.; Crimmin, M. R.; Barret, A. G. M.; Hill, M. S.; Kociok-Köhn, G.; Procopiou, P. A. *Organometallics* **2011**, *30*, 1493−1506. (b) Allan, L. E. N.; Clarkson, G. J.; Fox, D. J.; Gott, A. L.; Scott, P. *J. Am. Chem. Soc.* **2010**, *132*, 15308−15320.

(21) Eppinger, J.; Spiegler, M.; Hieringer, W.; Herrmann, W. A.; Anwander, R. *J. Am. Chem. Soc.* **2000**, *122*, 3080−3096.

(22) (a) Willey, G. R.; Woodman, T. J.; Drew, M. G. B. *Polyhedron* **1997**, *16*, 3385−3393. (b) Anwander, R. *Top. Organomet. Chem.* **1999**, *2*, 1−61.

(23) Hornillo-Martinez, P.; Hultzsch, K. C.; Hampel, F. *Chem Commun.* **2006**, 2221−2223.

(24) *SAINT+ NT version 6.04, SAX Area-Detector Integration Program*; Bruker AXS: Madison, WI, 1997−2001.

(25) Sheldrick, G. M. *SADABS version 2.03, a Program for Empirical Absorption Correction*; Universität Göttingen, Gottingen, Germany, 9197−2001.

(26) *SHELXTL version 6.10, Structure Determination Package*; Bruker AXS, Madison, WI 2000.

(27) Spek, A. L. *Acta Crystallogr.* **1990**, *A46*, C34.